



# Increased heating of the land surface as hot-dry events persist

Josephin Kroll<sup>1</sup>, Ruth Stephan<sup>1,\*</sup>, Andrew F. Feldman<sup>2,3</sup>, Diego G. Miralles<sup>4</sup>, and Rene Orth<sup>1</sup>

<sup>1</sup>Modeling Biogeochemical Systems, Faculty for Environment and Natural Resources, University of Freiburg, Germany

<sup>2</sup>Biospheric Sciences Laboratory, NASA Goddard Space Flight Center, Greenbelt, MD, USA

<sup>3</sup>Earth System Science Interdisciplinary Center, University of Maryland, College Park, MD, USA

<sup>4</sup>Hydro-Climate Extremes Lab, Ghent University, Ghent, Belgium

\* now at: Landkreis Breisgau-Hochschwarzwald, Freiburg, Germany

**Correspondence:** Josephin Kroll (josephin.kroll@ecoclim.uni-freiburg.de)

**Abstract.** Compound hot-dry events have devastating effects on ecosystems as well as societies. Combinations of more incoming shortwave radiation (SW<sub>down</sub>) and drying soil moisture lead to the build-up of high temperatures during dry periods. In this process, evaporation (ET) plays an important role in coupling temperature and soil moisture, and thus can lead to feedback loops and more drying. While both atmospheric contributors (SW<sub>down</sub>) and the land surface (ET) are known to influence temperature during dry periods, it remains unclear how their relevance for high temperatures varies throughout a dry event, i. e. from the build-up of heat to its persistence during ongoing dryness. Furthermore, the contributions of ET and SW<sub>down</sub> to heat onset and persistence during dryness are likely to differ across space and over the last decades. In this study, we investigate SW<sub>down</sub> and ET changes as two contributing factors to heat accumulation throughout dry events and across recent decades using reanalysis data. We determine periods of soil dryness accompanied by high temperatures using weekly timescale data. Within the detected hot-dry weeks, we distinguish between heat onset and heat persistence by evaluating the continuity of high temperatures. By mapping changes in ET and SW<sub>down</sub> during heat onset and heat persistence, we find that radiation increases contribute to the onset of heat globally but are less dominant for heat persistence. Evaporative cooling mitigates radiation-driven temperature increases during the onset of heat in humid regions. By contrast, this effect vanishes during persistent high temperatures. While the general occurrence of hot conditions during dry events increased from 14% to 28% from the 1980s to the 2010s, the evolution of ET and SW<sub>down</sub> throughout hot-dry events shows no clear trend over the last few decades. Our study emphasizes that contributors to heat development and/or persistence vary during the lifetime of a dry event which should be considered when analyzing compound extremes.

## 1 Introduction

Soil moisture extremes have been record breaking in the last two decades (Michaelian et al., 2011; Zou et al., 2018; Garrido-Perez et al., 2024; Kimutai et al., 2025). Various studies project an increase in drought frequency and intensity across several regions in the world, as summarized in the IPCC AR6 (Seneviratne, S.I. et al., 2023). While the impacts of extreme dryness are



devastating on their own, the compound occurrence with high temperatures adds additional stress on ecosystems, agriculture and societies (Bastos et al., 2020; Marchin et al., 2022; Leeper et al., 2025; Gu et al., 2025). At the same time, co-occurring  
 25 dryness and heat reinforce and amplify each other through land-atmosphere interactions by e.g. drought-driven increased heat advection and entrainment intensifying soil drying (Mueller and Seneviratne, 2012; Miralles et al., 2014; Gerken et al., 2018; Russo et al., 2019; Christian et al., 2020; Collazo et al., 2024).

Hot temperatures during drought can be induced via atmospheric and/or the land processes (Uckan et al., 2025). With regard to atmospheric processes, the shortwave downward radiation (SW<sub>down</sub>) that is not reflected provides energy that heats up  
 30 the surface. Depending on water availability, the incoming energy is partitioned mainly into latent heat flux (evaporation, ET) or sensible heat flux (H) (interplay illustrated in Figure 1 on the left side); in arid regions, increases in SW<sub>down</sub> primarily drive increases in H which increase the air temperature. This is also the case in humid regions but less pronounced, as in these energy-limited areas increased SW<sub>down</sub> simultaneously fuels latent heat flux which is reducing the energy diverted to H and thus warming (Yin et al., 2014). High levels of SW<sub>down</sub> at the surface are possible in the absence of clouds, which  
 35 at the same time correspond to a lack in water supply at the surface, i.e. precipitation, initiating dry-downs in the soil. Hence, atmospheric processes determine the joint development of higher temperatures and soil dryness through clouds modulating the amount of SW<sub>down</sub> reaching the surface and simultaneously determining precipitation and hence water supply. Also, land processes can contribute to hot temperatures during dry extremes (Seneviratne et al., 2010). With reducing soil moisture, ET is limited by water availability, and hence SW<sub>down</sub> is instead strengthening H, causing higher temperatures (Teuling, 2018). If  
 40 ET is not limited by water supply, a higher portion of SW<sub>down</sub> fuels latent heat flux, thereby leaving less energy for H and hence mitigating temperatures increases. A high contribution of the land surface to heat development has been shown to be associated with decreased water availability that leads to a shift from ecosystem energy- to water limitation (Whan et al., 2015; Hirschi et al., 2011; Zscheischler et al., 2015). However, the feedback between ET and soil moisture is not one-directional: while on the one hand soil moisture can limit ET, on the other hand ET amplifies soil moisture depletion by responding to  
 45 atmospheric water vapor demand (De Boeck and Verbeeck, 2011). Vapor pressure deficit corresponds to the deficit between saturation vapor pressure and partial vapor pressure. While saturation vapor pressure is only constrained by temperature, partial vapor pressure further depends on water availability. ET marks the process that balances the temperature-driven demand for water vapor in the atmosphere and water availability in the soil. Its magnitude depends on available energy (SW<sub>down</sub>), wind and vegetation activity next to demand (air temperature and dryness) and soil water availability (Seneviratne et al., 2010; Mueller and Seneviratne, 2012; Russo et al., 2019). In addition to these local-scale feedbacks, heat during drought is initiated or further amplified by several factors acting at larger spatial scales. For example, atmospheric circulation creates persistent weather patterns leading to the build-up of high temperatures (Brunner et al., 2017; Barriopedro et al., 2023). On a regional scale, advection of warm air can further increase temperatures during dry periods (Miralles et al., 2019; Schumacher et al., 2019) and secondly, diel dynamics in the local boundary layer support the persistence of high temperatures by trapping and  
 55 reintroducing warm air to the surface-near air (Miralles et al., 2014). These processes drive the state of the local atmosphere but are not explicitly explored in the following analysis.

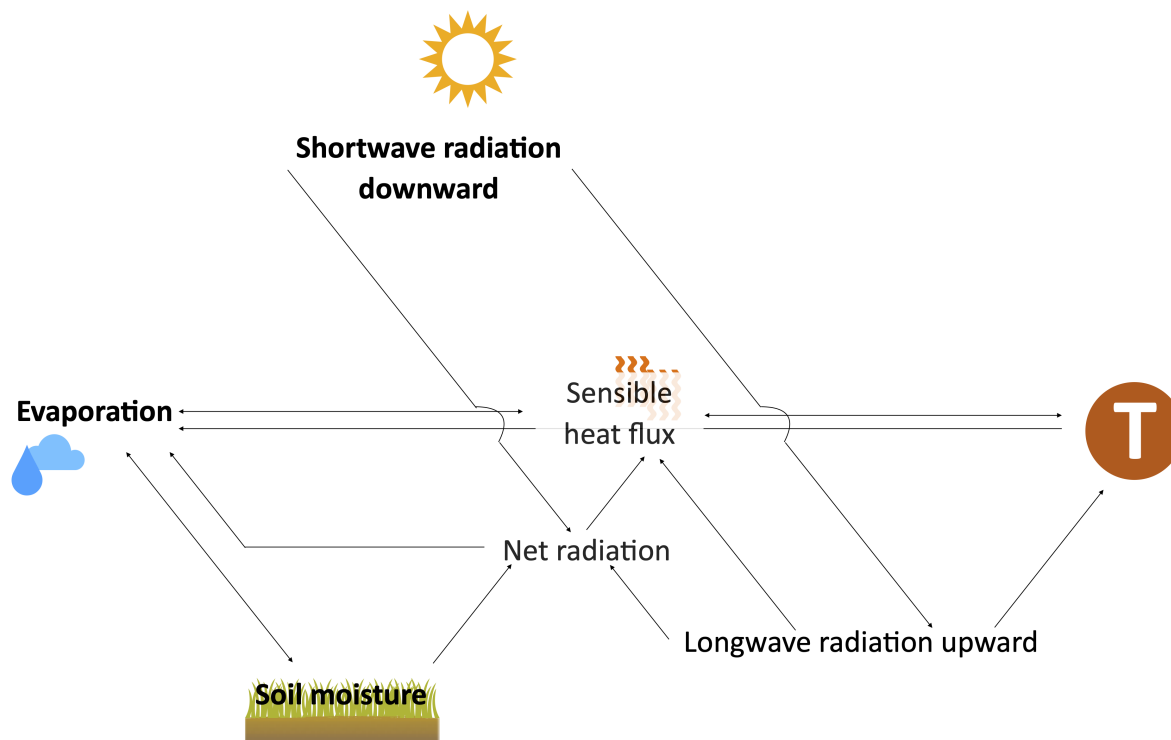


**Figure 1.** Schematic figure of the considered factors contributing to heat during dryness. Note that there are additional factors which have not been considered and are hence not displayed here.

However, the relative contributions of atmospheric processes (SW\_down) and land processes (soil moisture-constrained ET) to inducing hot temperatures during dryness remain understudied, in particular how their contributions vary in time, space and throughout dry events. This knowledge gap is relevant as it prevents the accurate inferring of the occurrence of compound hot-dry conditions in a changing climate. Under ongoing climate change, the simultaneous occurrence of high temperatures combined with severe decreases in soil moisture is projected to increase, leading to more extreme heatwaves (Teuling, 2018; AghaKouchak et al., 2020; Seneviratne, S.I. et al., 2023). Heat contributing factors are being altered such as large-scale circulation patterns (Brunner et al., 2018) as well as land-atmosphere feedbacks favoring dry and hot conditions (Seneviratne et al., 2006; Fischer et al., 2012; Stegehuis et al., 2013; Zscheischler et al., 2015; Vogel et al., 2017; Denissen et al., 2024). Additionally, long-term trends in soil moisture modify background climate and aridity and alter geographical patterns of ecosystem water or energy limitation (Vogel et al., 2018; Denissen et al., 2024). Furthermore, the last decades have been subject to ongoing land cover and land use change in many regions, transforming ecosystems and their responses to hot-dry conditions, as the albedo and transpiration capacity and hence net radiation (net\_rad), water and energy fluxes are modified (Alkama and Cescatti, 2016). Next to changes in ecosystem type and cover, rising carbon dioxide concentrations affect vegetation functioning and e.g. alter water demand (Keenan et al., 2013; Cheng et al., 2017) hence introducing changes in ET magnitude during normal



and extreme weather conditions.

In this study, we ask: How did the occurrence of compound hot and dry events change across recent decades? What is the relative importance of local atmospheric vs. land processes contributing to heat throughout the duration of dry periods? Did this vary across recent decades and in space? Specifically, we analyze the role of the local atmospheric forcing, represented by SW\_down, and that of the local land surface, represented by ET, in contributing to heat during dryness i) across recent decades; ii) across ecosystems and climate regions; and iii) throughout the lifetime of an event. We perform our analysis on a global scale to evaluate patterns across ecosystem and climate regimes. Additionally, we utilize data sets with a longer record from the 1980s–2010s to receive long-term trends in the importance of SW\_down and ET for heat during dryness. By distinguishing heat onset and heat persistence, we further clarify the relevance of SW\_down and ET throughout dry events.

## 2 Data and Methods

### 2.1 Data and Pre-processing steps

In this analysis, global reanalysis data with a 0.5° spatial resolution spanning the years from 1982 to 2021 is used to investigate heat contributors during dry events. We focus on SW\_down representing the atmospheric contribution and ET representing the land surface contribution. For enhanced understanding of the energy partitioning at the surface, we further investigate H, surface net\_rad and surface long-wave outgoing radiation (LW\_up). For all considered variables (see Table1), their data is averaged to weekly means. This temporal resolution covers dynamics of soil moisture (SM) and temperature adequately to allow the analysis of the evolution of heat and dryness while filtering out some shorter-term convective variability.

We focus on events outside freezing periods. Weeks considered as freezing and hence excluded are those when the average of the mean temperatures ( $t_{\text{mean}}$ , from ERA5 (Hersbach et al., 2020)) in the respective week and the two previous weeks is below 3°C. If this filtering results in a time series with < 50% of the weekly data points in a given analyzed decade, the grid cell is not considered in the entire analysis.

### 2.2 Methods

Our analysis framework includes several steps illustrated in Figure 2. Our study is carried out on a per decade basis to analyze long-term changes of heat drivers during dry periods across recent decades. The first considered decade is 1980–1989. As a first step, dry periods are identified. A weighted average of ERA5-Land SM across the top meter of the soil (layer 1–3) is computed (Muñoz-Sabater et al., 2021). From the weekly 40-year data record, percentiles are determined and used to assess the driest weeks as those with SM < 5th percentile. The dryness peak is the week in which SM is lowest, see Figure 2 labeled as "Peak". For each dry peak detected this way, we define the start of the dry-down as the week before the driest peak in which SM was exceeding the 10th percentile, labeled as "Start" in Figure 2.

Within the detected dry periods, the occurrence of hot weeks is determined. Using ERA5 maximum temperature (Hersbach





et al., 2020) ( $t_{max}$ ), hot weeks are defined based on the weekly 40-year data record as weeks with a temperature  $\geq 95$ th percentile. Then, the occurrence of hot weeks during dry periods is described as the number of hot weeks within the dry event over the number of weeks between dry period start and peak.

$$\% = \frac{N_{hot\ weeks}}{N_{dry\ weeks}} * 100 \quad (1)$$

Furthermore, we distinguish whether a hot week marks the onset of high temperatures or is part of a persistent episode of high temperatures to study potential differences in the heat-inducing vs. heat-sustaining mechanisms. The differentiation between 'heat onset' and 'heat persistence' is based on the continuity of high temperatures: If during more than one week prior to a hot week, temperatures are  $< 95$ th percentile, the hot week is considered as heat onset, labeled as circles in Figure 2. If exactly one week or less is between the hot week and a previous hot week, the hot week is considered as heat persistence, labeled as filled circles in Figure 2. Consequently, there can be more than one heat onset during a dry event. The applied methodology for detecting dry extremes is illustrated in Step 1 in Figure 2

In a next step, we aim to study the mechanisms introducing heat during dry events. For this purpose, the dynamics of selected controlling factors of heat are considered in form of week-to-week changes in absolute numbers (Step 2 "Analysis of heat contributors" in Figure 2):

$$\Delta X = X_t - X_{t-1} \quad (2)$$

In the equation X refers to the selected heat driver such as ET or SW<sub>down</sub>, while t refers to the index of a detected hot week. These changes of heat drivers from one week to the next are calculated for both heat onset weeks and heat persistence weeks in each decade in order to analyze potential differences and related long-term trends. As week-to-week changes refer to a change relative to the previous week this means in the case of persistent hot-dry conditions changes in variables can be relative to a week i) when heat sets on (as depicted in Figure 2 Box ("detect hot conditions during dryness), ii) which is only dry but follows a hot week and iii) already characterized by persistent hot-dry conditions. Finally, the relevance of heat drivers is analyzed across space to find potential variations alongside patterns of long-term dryness and tree cover fraction. long-term dryness is computed as the ratio of unit-adjusted precipitation (precip) (Allen et al., 1998) over net<sub>rad</sub>. Tree cover fraction is gathered from the Vegetation Continuous Fields (VCF) product based on observations with the Advanced Very High Resolution Radiometer (AVHRR) (Hansen, M.,).

### 3 Results and Discussion

#### 3.1 Trends in the occurrence of hot-dry extremes across recent decades

As a first step, the percentage of hot weeks during dry periods is determined for every decade, respectively (Figure 3). Over the considered time period, the percentage of a dry event which is hot increases in many regions, with the global median increasing from 14% to 28%. This agrees with Manning et al. (2019) who found an increased probability of hot-dry events over the period

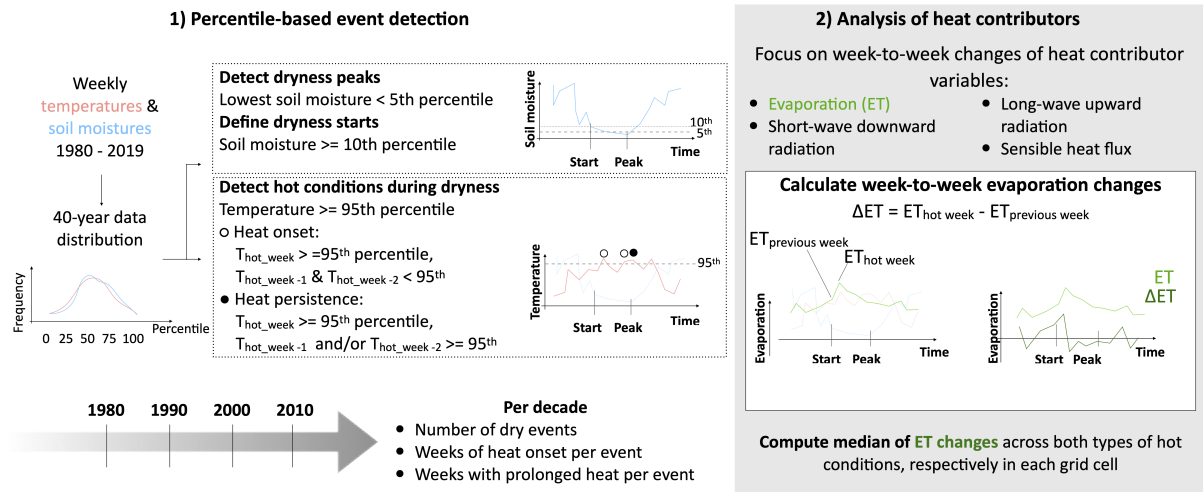


**Figure 2.** Illustration of our methodological approach. The calculation in part 2 on the right is illustrated for ET and performed similarly for the other heat contributor variables.

**Table 1.** Data sets used in this study. Variable names correspond to the abbreviations used here and therefore might differ from abbreviations in the original data sets (long-wave surface radiation downwards LW\_down, net long-wave surface radiation LW\_net, fractional vegetation cover FVC).

Data set	Version	Variables	Application	Reference
GLEAM	4.2a	ET, H	Heat contribution	Miralles et al. (2025)
ERA5		t_max, t_mean, SW_down, LW_down, LW_net, net_rad, precip	Heat detection Freezing filter Heat contribution Dryness regimes	Hersbach et al. (2020)
ERA5-Land		SM1-3	Dry event detection	Muñoz-Sabater et al. (2021)
VCF		FVC	Tree cover regimes	Hansen, M.,
Fluxcom-X-Base		ET	Heat contribution	Nelson et al. (2024)
SoMo.ml	v1	SM1-3	Dry event detection	O and Orth (2021)

of 1950–2013. Also modelling studies predict higher temperatures due to stronger SM constraints in the future (Rasmijn et al., 2018; Denissen et al., 2024). The overall increase shows strong regional differences with northern South America, southeast Asia and southern Africa as hot spots of increases in high temperatures during periods of low SM. It is tested whether the increase in the percentage of hot weeks during dry periods is induced by long-term trends in temperature. For this purpose, the percentile-based thresholds for dryness and heat are re-calculated based on the data within each decade instead of the entire 40-year record. This approach yields a different picture: The percentage of dry events that is accompanied by hot temperature



140 increases from the 1980s to the 2010s, but far less from 20% to 22% (Figure SA1). This suggests that the increase in the percentage of hot weeks during dry events is induced mainly by climate-change driven changes in temperature and SM, while drought-related processes modulating hot extremes and heatwave-related processes modulating droughts play a more limited role.

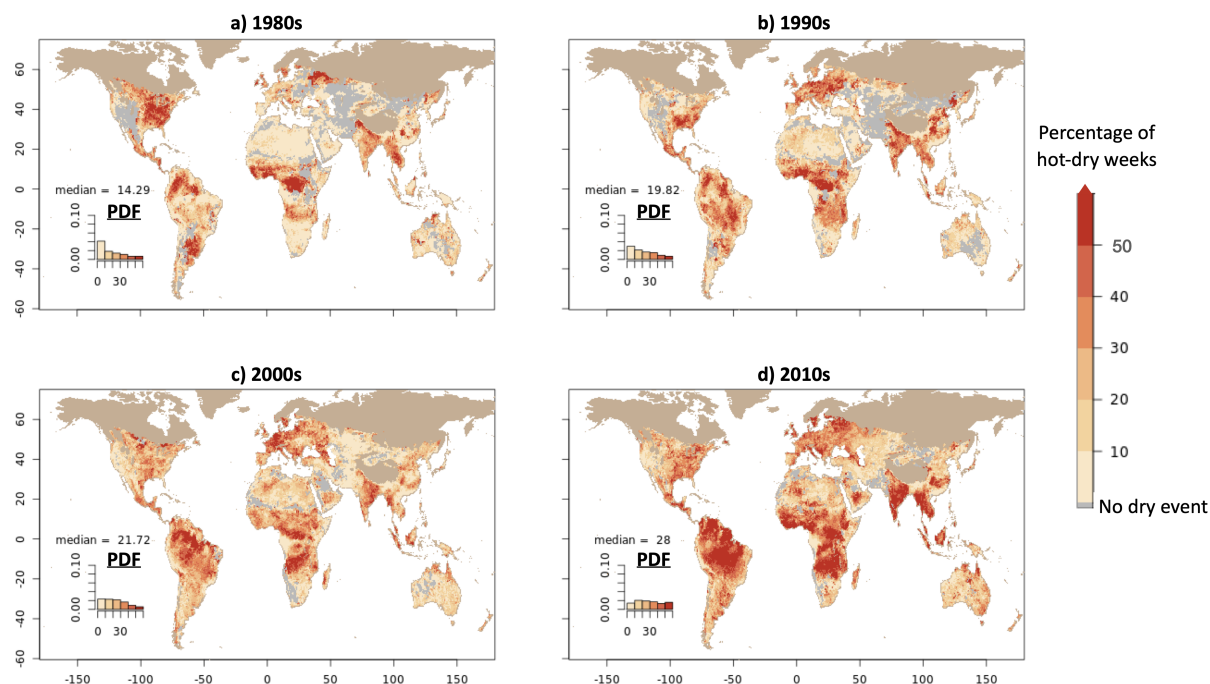


**Figure 3.** Percentage of hot weeks during dry events. Maps show the median across all local dry events. PDF refers to probability density function of the displayed grid-cell values.

### 3.2 Drivers of heat onset during dryness

145 Next, the effect of the local atmosphere and land drivers is explored throughout the identified dry events using SW\_down and ET, respectively, as diagnostics. For one example decade (2010s), the week-to-week changes in SW\_down and ET during hot-dry weeks are summarized for both heat onset and persistent heat (Figure 4). At the onset of heat, strong increases in SW\_down are found across large areas (see Figure 4a). SW\_down decreases only in a few, mainly dry areas as western US, western Asia, northeastern Africa and South Australia. Net\_rad largely follows this pattern (see Figure S A2e), suggesting that

150 increases in SW\_down translate largely directly into energy available for H and ET. In the subsequent paragraphs we therefore focus on week-to-week changes in SW\_down instead of net\_rad changes during hot-dry events. Exemptions where net\_rad does not follow SW\_down exist e.g. in western US and parts of southern Australia, where strong increases in LW\_up can be found. Although SW\_down and hence available energy increases largely, ET and H show spatially varying responses (see



Figure 4c and Figure S A2g, respectively). We find hot spots in which ET increases in northern South America, eastern US and central Europe. ET decreases are strongest in western US and western Asia, southern South America. As ET is driven by both SW<sub>down</sub> and SM, we illustrated in Figure S A3a the simultaneous changes of all the three variables to pinpoint where ET follows the signal of available energy vs. available water. In central Europe, the eastern US and core parts of the tropical regions,  $\Delta ET$  and  $\Delta SW_{down}$  agree on the sign, while the week-to-week change in SM is opposite. In India, eastern Africa and central South America ET follows changes in SM. Lastly, there are regions where ET, SW<sub>down</sub> and SM change in the same direction. Temperature increases overall (see Figure S A2a), however regions like central Europe, southern South America and southern Australia show high magnitudes in the week-to-week change during the onset of heat during dry events. Aggregating week-to-week changes in ET and SW<sub>down</sub> along long-term dryness and tree cover classes as in Figure 5b, d reveals that increases in SW<sub>down</sub> are strongest in humid regions, while they are weaker in semi-arid and arid regions. For ET, the gradient in long-term dryness has an even stronger influence, as from week-to-week ET increases in humid regions, while it decreases in arid regions. For semi-arid regions the change in ET depends on the tree cover fraction: higher tree cover corresponds to less negative or even positive changes in ET. Our findings suggest that due to the dissipation of clouds after former cloudy conditions or rainfall events, SW<sub>down</sub> increases widely causing the onset of heat during dry periods, which was found for Europe as well by De Boeck and Verbeeck (2011). Increased SW<sub>down</sub> translates in a main part of the globe into higher levels of net<sub>rad</sub>. However, in a few cases net<sub>rad</sub> declines with the onset of heat during dryness due to a dominating influence of changes in LW<sub>up</sub>. Declining net<sub>rad</sub> during hot-dry events was also found across some regions in O et al. (2022). long-term dryness determines the intensity of SW<sub>down</sub> increases and the direction of ET changes. Likely due to the higher variability of SW<sub>down</sub> in humid regions week-to-week changes in those areas are of higher magnitude compared to week-to-week changes in semi-arid and arid regions. The contrasting ET changes between humid and arid regions during the onset of heat during dryness correspond well with the concept of ecosystem water- vs. energy limitation: In energy-limited, or humid ecosystems, an increase in SW<sub>down</sub> leads to increases in H and ET as water availability is sufficient, with the net effect leading to mild temperature increases (Yin et al., 2014; Teuling et al., 2013; Benson and Dirmeyer, 2021). Contrary, in water-limited, so arid systems increases in SW<sub>down</sub> cannot fuel ET as water availability limits the process leading to larger H and thus temperature increases. The contrasting change of ET between humid and arid regions over the course of a dry event is also highlighted in O et al. (2022). Vicente-Serrano et al. (2020) emphasize the high vapor pressure deficit that develops in drier areas during hot-dry periods, which can next to soil moisture limitation additionally suppress ET from a stomatal point of view.

The influence of tree cover on week-to-week changes in SW<sub>down</sub> and ET is compared to long-term dryness rather low during the onset of heat during dryness. In humid regions the ET response depends on small-scale species-specific aspects and site-dependent characteristics as e.g. water table depth and soil type (Zha et al., 2010; Thom et al., 2023) and might therefore by hardly visible in the spatially aggregated visualization. However, along a tree cover gradient in semi-arid regions, week-to-week ET changes vary gradually as well which might be related to the fact that trees can access deeper layers of water and hence sustain transpiration despite overall dry soils (Feldman et al., 2023), while grasses are highly dependent on shallow SM (Zha et al., 2010). Consequently, temperature increases during dryness are caused by increased H which results either



i) from increases in SW<sub>down</sub> as e.g. in humid regions like central Europe or ii) from increased SW<sub>down</sub> in combination  
 190 with SM-constrained ET as e.g. in drier regions like southern South America. Furthermore, there are exemptions where we  
 can see strong week-to-week temperature increases during dryness although net<sub>rad</sub> and subsequently H and ET decline as  
 in southern Australia. Here, other not considered drivers of high temperatures e.g. advection or large-scale circulation might  
 play an important role. Independent of what causes the temperature increases resulting from increased H during dryness — i)  
 increases in SW<sub>down</sub>, ii) SW<sub>down</sub> increases in combination with SM-suppressed ET or iii) other factors — magnitudes are  
 195 comparable. As a next step the week-to-week changes in SW<sub>down</sub> and ET are compared across the first and last decade in  
 Figure 5 a and b, c and d, respectively; stronger SW<sub>down</sub> increases during heat onset are found in most humid and semi-arid  
 regions in recent times. week-to-week changes of SW<sub>down</sub> in arid regions stay similar across decades. In humid regions, ET  
 increases during the onset of heat grow in magnitude over the decades, while they decrease in magnitude in semi-arid regions  
 with high tree cover. In semi-arid regions with low tree cover and across arid regions, ET changes during the onset of heat stay  
 200 rather constant over the decades. The stronger increases in SW<sub>down</sub> during the onset of heat in dry periods in the 2010s could  
 be affected by less aerosols in the atmosphere (Xu et al., 2018; Zhao et al., 2019). Additionally, reduced cloud cover in the  
 tropics (Duku and Hein, 2021; Leite-Filho et al., 2021; Xu et al., 2022) and hence less SW<sub>down</sub> being absorbed or reflected in  
 higher altitudes of the atmosphere could cause SW<sub>down</sub> increases of higher magnitude in humid regions in the 2010s. Weaker  
 increases in ET or decreases in semi-arid regions along a tree cover gradient in the 2010s compared to the 1980s suggest that  
 205 either vegetation is more affected by water limitation during dry periods due to higher event severity or higher sensitivity of  
 vegetation to water deficits (Li et al., 2022). At the same time, higher atmospheric evaporative demand in a warmer climate, or  
 increased water use efficiency due to CO<sub>2</sub> fertilization (Keenan et al., 2013; Cheng et al., 2017) may play a role in reducing  
 the magnitude or switching the direction of ET changes over the decades. Overall, the small magnitudes of changes from the  
 first to the last decade suggest that factors other than dryness-related processes modulating hot extremes might play a more  
 210 important role for the long-term increase in compound hot-dry extremes. This aligns well with our finding from Figure 3 that  
 the increasing trends in the co-occurrence of hot and dry conditions over time is largely associated with long-term trends in  
 SM and temperature.

### 3.3 Drivers of heat persistence during dryness

215 In the subsequent paragraphs the role of local heat drivers as SW<sub>down</sub> and ET during the persistence of heat during identified  
 dry events is evaluated (see Methods section: persistence of heat during dryness refers to conditions in which between a hot  
 week and a previous hot week there is a maximum of one week with temperatures below the 95th percentile). During persistent  
 hot-dry conditions, SW<sub>down</sub> decreases globally except in low latitudes (see Figure 4b). However, the magnitude of week-to-  
 week changes is small compared with those during the onset of heat during dry events, especially in the low latitudes. week-to-  
 220 week changes in net<sub>rad</sub> show a similar spatial distribution, although of smaller magnitude than SW<sub>down</sub> changes (see Figure  
 SA2f). Differences between SW<sub>down</sub> and net<sub>rad</sub> occur in mainly in central Africa and India, where changes in SW<sub>down</sub>  
 are of small magnitude and hence similar to changes in LW<sub>up</sub>. week-to-week changes in ET show smaller magnitudes during

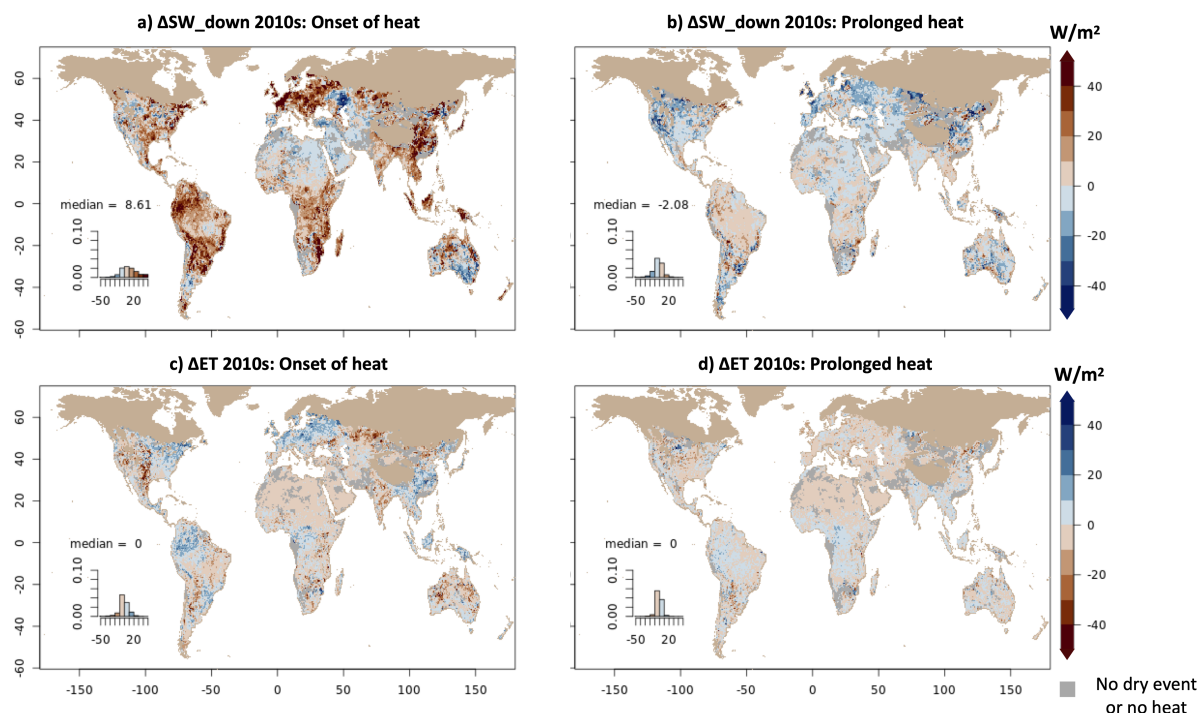


**Figure 4.** Median week-to-week changes of SW\_down and ET during the onset of heat (a, c) and during persistent heat (b, d) within dry events in the 2010s.

the persistence of heat (see Figure 4d). ET declines across most parts of Europe, northern Africa, central US as well as western Asia. In contrast, ET increases in the core tropical regions. Across most regions globally during persistent heat conditions, ET co-varies from week to week with both SW\_down and SM (see Figure S A3). The temperature changes related to SW\_down and ET changes during persistent heat are positive in most regions, but show a smaller magnitude compared to the onset (see Figure SA2b). The temperature increases are largest in areas where SW\_down decreases most strongly, e.g. central Europe and southern South America. The spatially aggregated results of week-to-week changes in SW\_down and ET during persistent hot-dry conditions show a high similarity between humid and arid regions, especially compared to the onset of heat during dryness (Figure 6b, d). Furthermore, the week-to-week changes of both heat contributors are overall much smaller. week-to-week changes in SW\_down neither vary strongly along a tree cover percentage gradient nor along a long-term dryness gradient. However, week-to-week changes in ET vary more strongly along the tree cover percentage and long-term dryness gradient. The strongest decreases in ET during the persistence of heat, can be found in regions with a long-term dryness of 0.5 – 1. In strongly humid areas (long-term dryness < 0.5), ET stays constant or slightly increases across all tree cover regimes. For semi-arid and arid regions, ET declines rather weakly within a period of persistent heat during dryness. Across humid and semi-arid regions, changes in ET become less negative or even positive with higher tree cover percentage. Small increases or even decreasing SW\_down during the persistence of heat during dryness may be related to the fact that SW\_down is already

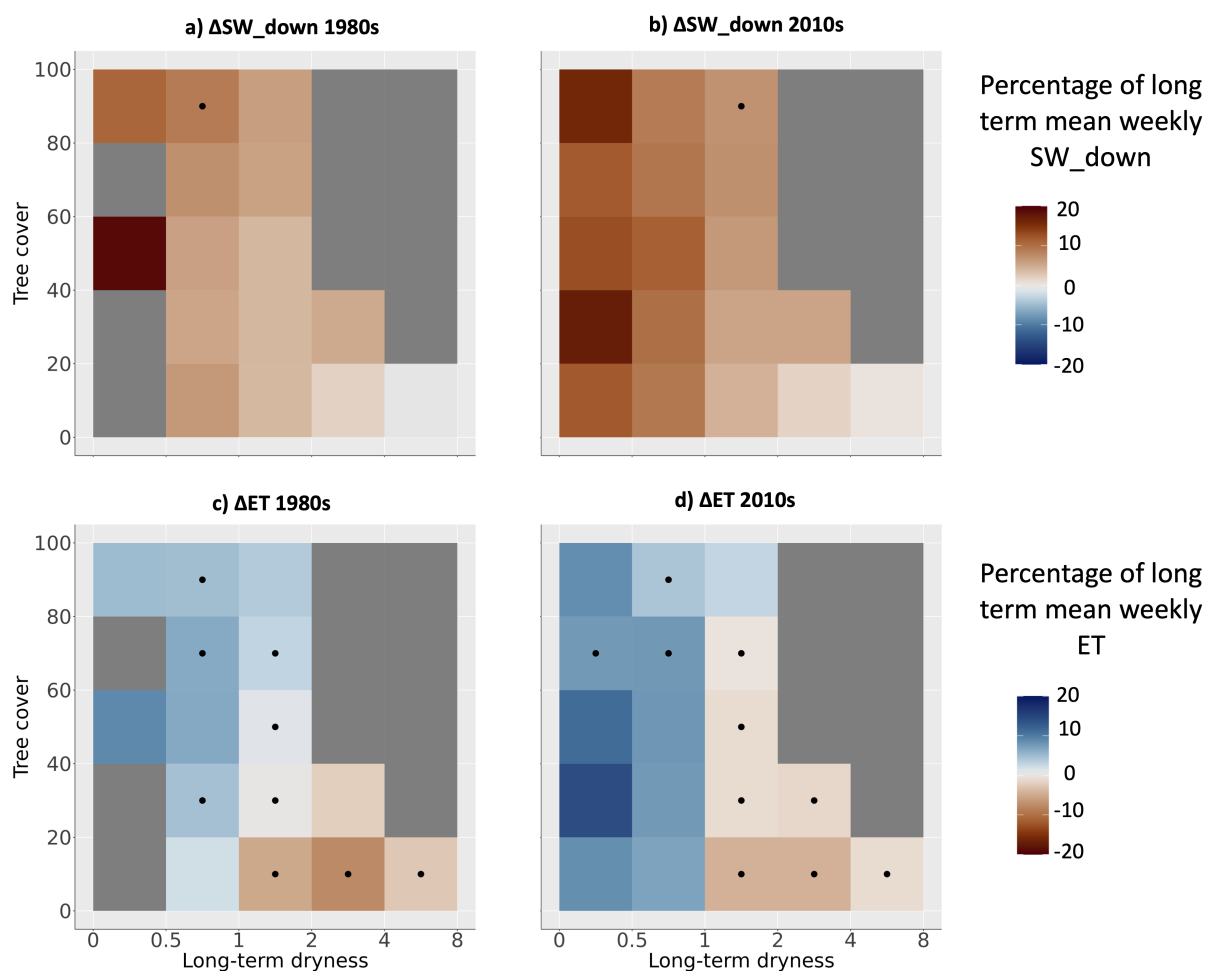


**Figure 5.** Week-to-week changes in SW\_down and ET during heat onset (relative to 40-year long-term weekly mean). Calculated as median across all grid cells in tree cover-dryness classes. long-term dryness refers to the ratio of unit-adjusted precipitation over net\_rad, increasing values therefore depict drier regimes. Dots indicate the standard deviation of normalized data in a respective tree cover-dryness class to be less than 20% of the mean displayed by the color. Results shown for 1980s and 2010s. Note that considered grid cells grouped into a tree cover-dryness class might shift between decades, as they may experience dry extremes and heat only in one of the decades. Grey boxes indicate less than 50 grid cells within the tree cover-dryness class.





at very high levels during heat onset and has a limited ability to increase further. The decreases in SW<sub>down</sub> also might reflect minor cloud cover arriving ahead of the following rain events that end the dry spell. Comparing week-to-week ET changes during the onset vs during the persistence of heat during dryness, the strongest differences become apparent in regions with a long-term dryness of 0.5–1. While during the onset of heat, these regions showed increases in ET, during heat persistence they experience decreases in ET. This could either be a sign of regions with a long-term dryness of 0.5–1 becoming water-limited during persistent hot-dry conditions and declining ET as a result. This explanation is supported by the fact that temperature increases during heat persistence are largest in rather humid areas as central Europe and southern South America, which could be related to reduced evaporative cooling. Alternatively, also decreasing SW<sub>down</sub> could cause ET to decrease. The positive effect of increasing tree cover on week-to-week ET changes in humid regions might be related to the fact that trees can access deeper water layer and hence sustain ET despite experiencing longer lasting hot-dry conditions (Feldman et al., 2023; Zha et al., 2010). Overall, the relatively small contributions from SW<sub>down</sub> and ET to the sustained high temperatures or even further temperature increases suggest that there other relevant processes such as advection (Miralles et al., 2019; Schumacher et al., 2019) or vertical entrainment (Miralles et al., 2014) playing a role for the persistence of high temperatures during dry periods. As a next step, the week-to-week changes of SW<sub>down</sub> and ET during persistent hot-dry conditions are compared between the 1980s and 2010s (see Figure 5 a and b, c and d, respectively): SW<sub>down</sub> increases stronger in the 2010s compared to 1980s in regions with 80–100% tree cover. ET decreases stronger during persistent heat in the 2010s. While in the 1980s, an increase in tree cover percentage aligned with more positive ET changes in regions with a long-term dryness of 0.5–2, in the 2010s ET increases in those regions only if the tree cover percentage is between 80–100%. As previously suggested stronger increases in SW<sub>down</sub> during the persistence of hot-dry conditions could be related to a generally decreased cloud cover, especially in the tropics (Duku and Hein, 2021; Leite-Filho et al., 2021; Xu et al., 2022). The development towards overall negative week-to-week ET changes during persistent hot-dry conditions from the 1980s towards the 2010s could be due to climate change leading to higher temperatures during heat phases in the end of the study period (Dunn et al., 2020). This could potentially cause more heat stress for vegetation, vapor pressure deficit increases and hence stronger reductions in evaporative cooling. As a final step in our analysis, the temporal evolution of changes in evaporation during the course of dry events is analyzed in Figure 7. Dry events increase in length from humid over semi-arid to arid regions. This has to do with the reduced variability of SM in response to less precipitation (variability). However, the percentage of area affected by dry conditions accompanied by heat (onset and persistence) is generally higher in humid and semi-arid regions compared to arid regions as listed in table 2. This is probably related to overall higher ET and a corresponding stronger role of ET in connecting dryness and heat outside arid regions. ET is mostly changing at heat onset and changes are much smaller for heat persistence, as discussed also above. Also, contrasting ET changes are confirmed between humid and semi-arid regions, illustrating the effect of SM limitation on ET in the semi-arid regions.

Figure 7 was repeated with alternative SM and ET data, respectively, from SoMo.ml (weighted mean across the top 50cm of the soil) (O and Orth, 2021) and Fluxcom X-Base (Nelson et al., 2024). Because of the shorter time period covered by these data sets, percentile-based thresholds for dryness and heat are calculated based on the data of one decade (2010-2019). The results show similar time evolution of week-to-week changes of ET during dry events Figure S A4 underlining the robustness

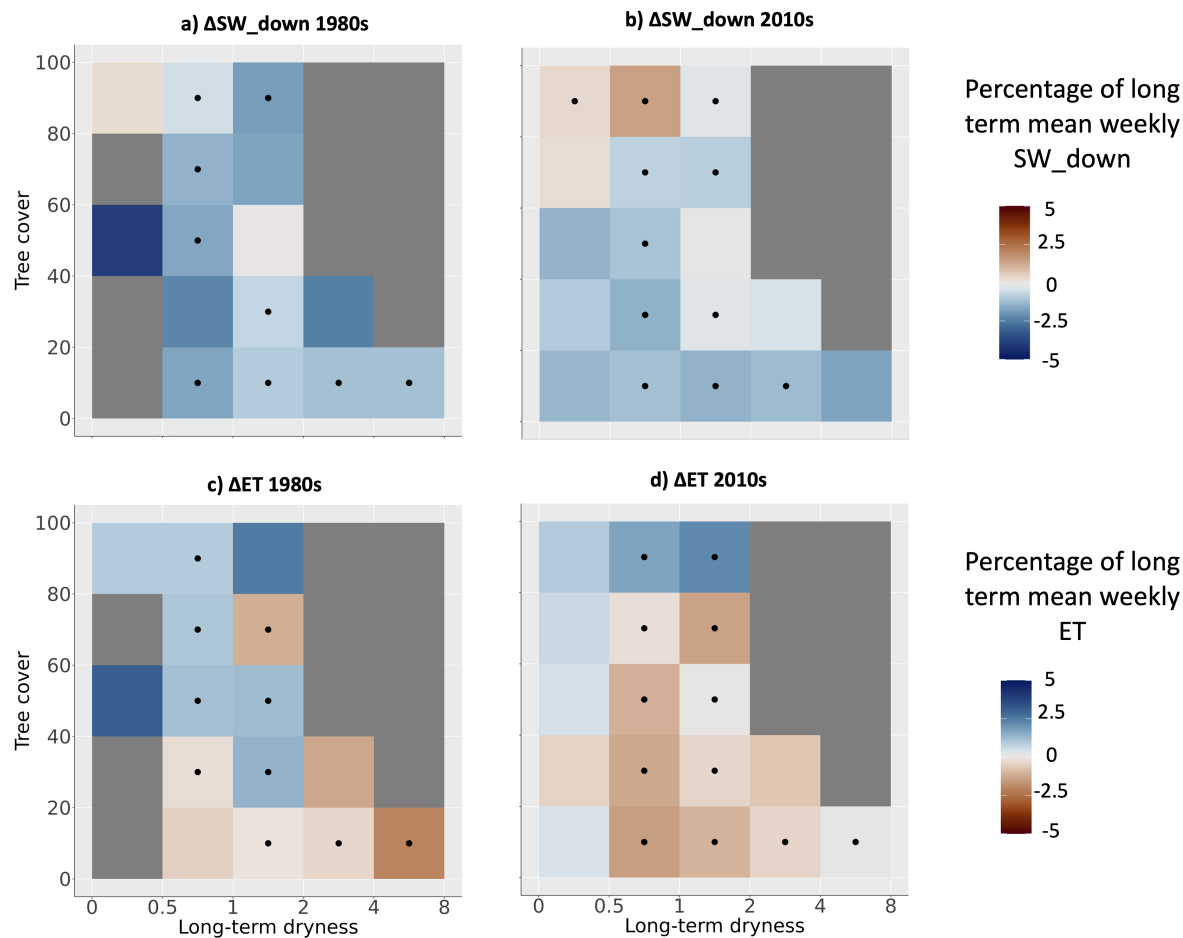


**Figure 6.** Similar to Figure 5 but for persistent heat during dry events.

**Table 2.** Percentage of area in humid, semi-arid and arid regions affected by dry–no heat or hot-dry conditions.

		Humid regions	semi-arid regions	Arid regions
10 weeks before peak	Dry–no heat	74	78	80
	hot-dry	26	22	20
5 weeks before peak	Dry–no heat	63	67	78
	hot-dry	37	33	22
During dryness peak	Dry–no heat	50	55	71
	hot-dry	50	45	29

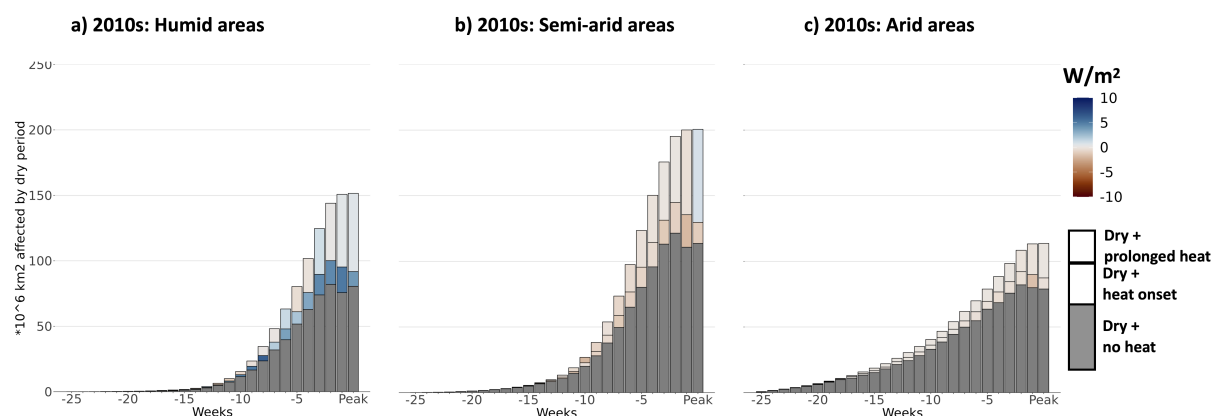


**Figure 7.** Time evolution of week-to-week changes of ET during dry events. Results expressed as area affected by dry extremes in (a) humid (long-term dryness index  $< 1$ ), (b) semi-arid (long-term dryness index  $= 1-2$ ) and (c) arid regions (long-term dryness index  $> 2$ ). Area is aggregated across space (affected grid cells in respective dryness regime) and time (number of events in each grid cell). Results calculated as median value across all events for the same weeks relative to the event peak.

of the overall results based on reanalysis data. There is some discrepancy in terms of the fraction of the area which is affected by heat in addition to dryness. This is smaller in the analysis with the alternative datasets, probably related to the fact that in the main analysis maximum temperature and SM data were derived from the same data set (ERA5) such that a higher coincidence of dryness and high radiation and hence temperatures can be expected.

### 3.4 Sensitivity to methodological choices

The percentile-based identification of dry and hot extremes applied in this study allows capturing locally relevant periods of soil dryness or heat. However, the detected events are not comparable across different regions in terms of absolute soil moisture nor temperature. The choice to base the event detection on soil water content ensures that periods with relatively low moisture are detected. This does not mean that vegetation and hence ET are actually affected everywhere as such impacts are linked to the absolute soil moisture content rather than the relative content, i.e. even if soils are relatively dry in a wet region they may still provide sufficient water for vegetation functioning.

The threshold to determine dry period peaks is the 95th percentile for the local 40-year soil moisture data distribution. Therefore, detected events in dry regions are very likely to happen in the dry season, when vegetation is less active. This affects the detectable changes in ET as the variability of ET is reduced in these periods. Future research may revisit our analysis with different percentile thresholds for the soil moisture dryness identification, i.e. for mild droughts which are more likely to occur outside the dry season and hence could actually have stronger impacts on vegetation in dry regions.

The event detection is further based on soil moisture during the event peak being below the 5th percentile. Other factors representing event severity e.g. accumulated water deficit, dry period length, or dry-down speed are not considered in the event detection. While outside the scope of our study, these aspects might influence the vegetation and ET response and consequently



the determined importance of ET during heat. Next to the event-specific characteristics, also the vegetation status influences ET variability and thus its potential for evaporative cooling during heat. Legacy effects of previous dry periods might affect the ability and magnitude of vegetation responding to a recurring period of water limitation.

295 Lastly, excluding other direct drivers of heat such as advection and vertical entrainment comes leads to the situation that we can not fully explain hot temperature occurrences and dynamics. However, we can still infer the (non-) relevance of ET and SW\_down. The determined changes of ET and SW\_down allow to explain the the onset of heat during dryness to a large extent in our results, suggesting minor relevance of advection and entrainment in many regions.

#### 4 Summary and Conclusions

300 In this study, we focus on contributors to and characteristics of hot temperatures during dry events.  
 By investigating dry periods in four subsequent decades, we can show that the percentage of dry events that is accompanied by high temperatures increases from 14% to 28%. Despite the more frequent co-occurrence of heat and dryness, our analysis of incoming radiation, representing the atmospheric contribution and evaporation, exploring the land contribution to heat during dryness, reveals no clear long-term trend since the 1980s.

305 Through the differentiation between heat onset and heat persistence during dryness, we demonstrate that the relevance of heat contributors changes throughout dry events. Incoming radiation has a high relevance for the onset of high temperature globally during dry periods, but not for the persistence of hot-dry conditions. In contrast, increased evaporation can mitigate the onset of high temperatures in humid regions, but this effect vanishes in semi-arid and arid regions and during persistent hot-dry conditions and hence supports higher temperatures. This is inline with several other studies that find breakpoints  
 310 in the contribution of evaporation to temperature related to dryness (Hirschi et al., 2011; Teuling et al., 2013; Benson and Dirmeyer, 2021). Our findings open up the question which other factors next to reduced evaporation contribute to persistent high temperatures during dry conditions.

The usage of week-to-week changes to determine the relevance of the local atmospheric vs land contribution to heat onset and persistence enabled us to pinpoint when which hydro-meteorological variables change most. Our approach emphasizes the  
 315 advantage of looking at shorter time-scale changes instead of individual time steps, yielding information about the dynamics in contributor and target variables.

In the light of ongoing climate change the role of evaporation in influencing temperatures during dry events might change as the water demand of the atmosphere increases, in turn driving evaporation especially under conditions of extreme temperatures and dryness. Additionally, land use is changing altering ecosystem characteristics which connects back to dynamics in evap-  
 320 oration and incoming energy by e.g. changes in cloud cover and aerosols (Alkama and Cescatti, 2016; Duku and Hein, 2021; Leite-Filho et al., 2021; Xu et al., 2022). All these changes have the potential to modify the role of evaporation and incoming energy in contributing to heat during dryness.



*Code and data availability.* The data used in this study is publicly available. The code for the analysis will be made available in a Zenodo Archive upon publication.

## 330 **Appendix A**

### **A1**

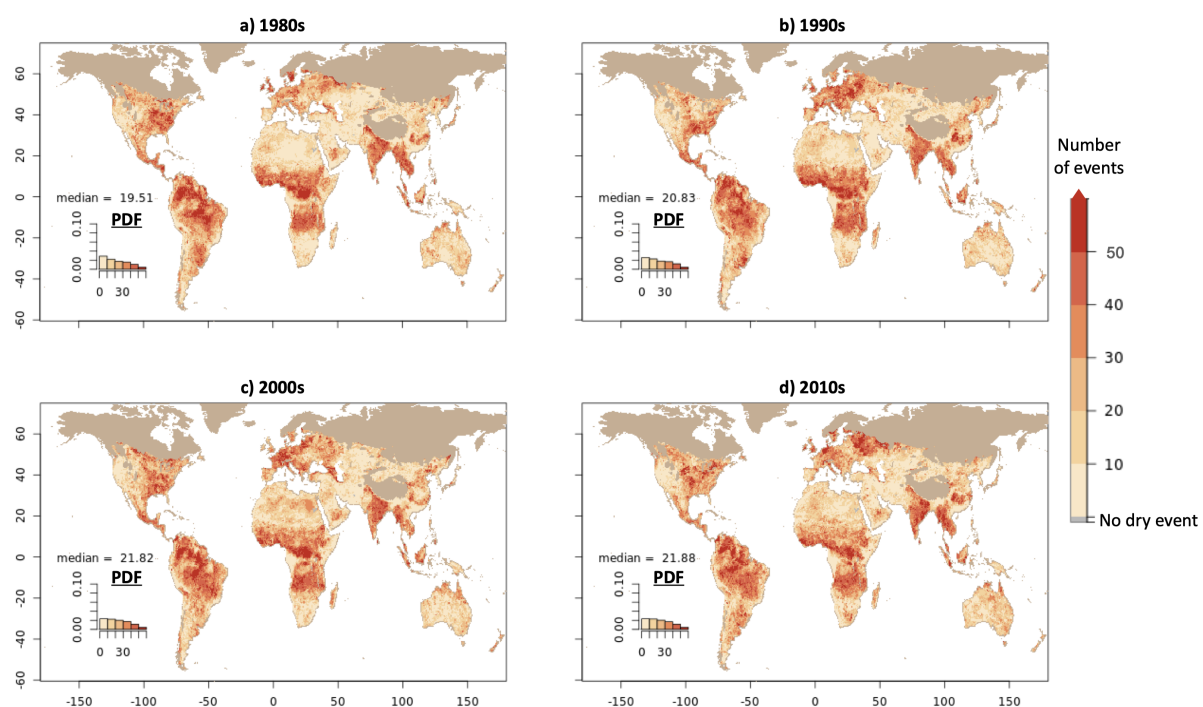


**Figure A1.** Percentage of hot weeks during dry events with percentile-based thresholds of SM and  $t_{\max}$  being calculated for each decade separately. Maps show the median across all local dry events. PDF refers to probability density function of the displayed grid-cell values.

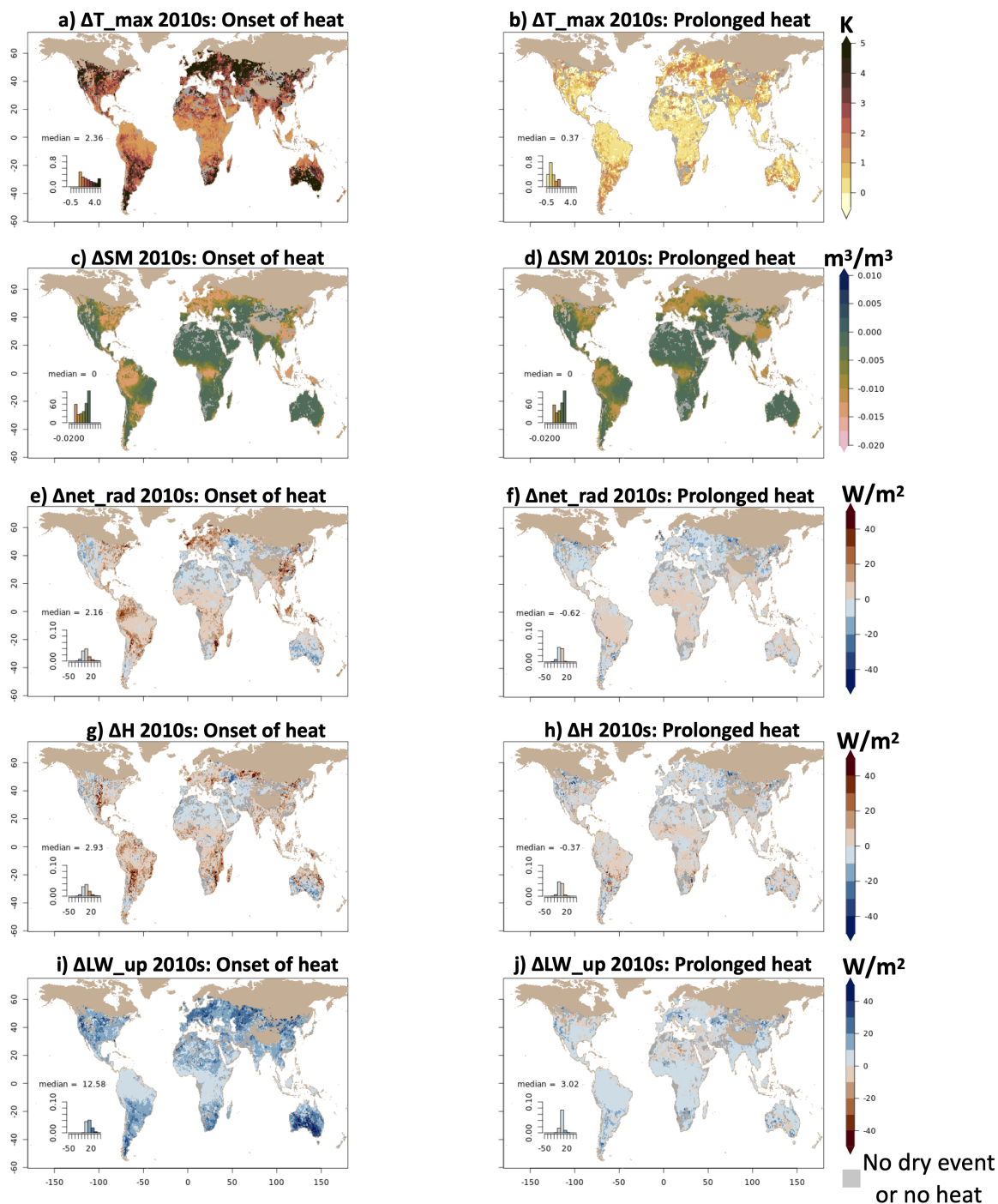


**Figure A2.** Median week-to-week changes of  $t_{\max}$ , SM,  $net\_rad$ , H and  $LW\_up$  during the onset of heat (a, c, e, g) and during prolonged heat (b, d, f, h) in the 2010s. Barplots in the lower left corner of each panel depict histograms of the probability density functions of the grid cell values.



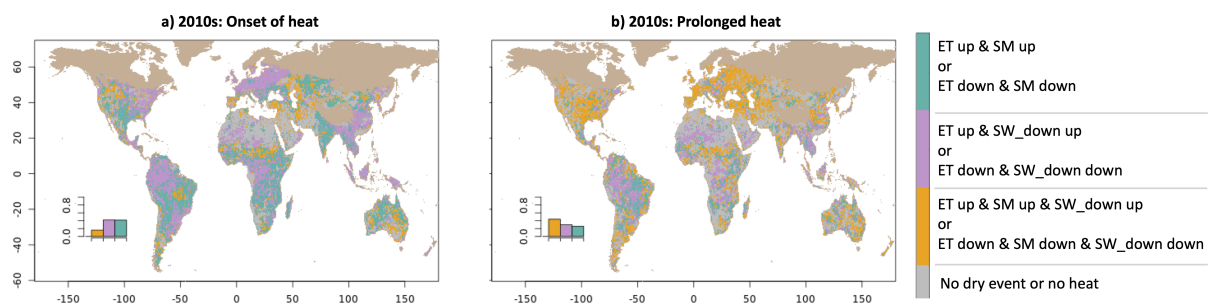


**Figure A3.** Similarity of week-to-week changes in ET with changes in SM and SW\_down, respectively during the 1980s and 2010s.

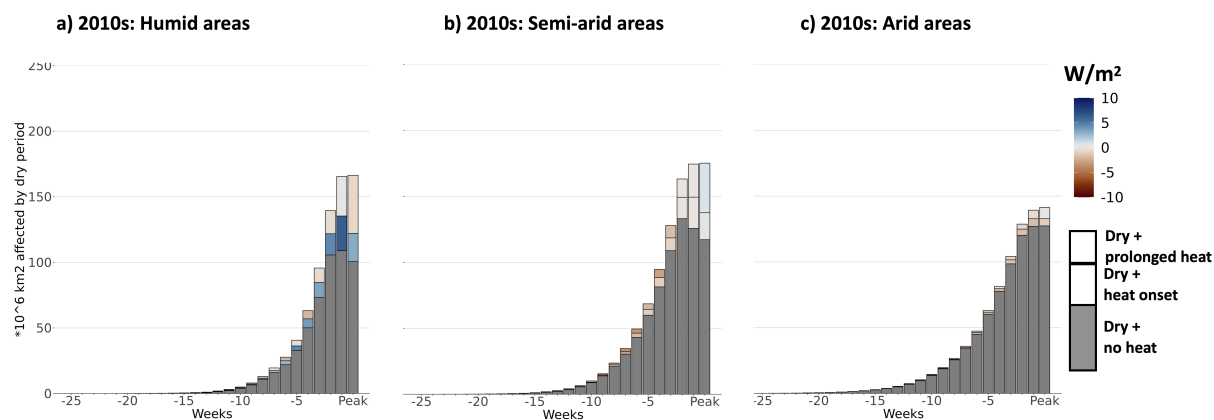


**Figure A4.** Similar to Figure 7 but based on SM data from SoMo.ml O and Orth (2021) and ET data from (Nelson et al., 2024) and thresholds for heat and dryness defined based on a 10-year data distribution from 2010–2019.



*Author contributions.* J.K., R.O. and R.S. jointly designed the study. J.K. performed the analysis and drafted the manuscript. All authors discussed and interpreted the results and improved the manuscript.

*Competing interests.* The authors declare that they have no conflict of interest.

*Acknowledgements.* We thank the Modelling of Biogeochemical Systems group at University of Freiburg for fruitful discussions and constant support. Specifically, we thank Hao Huang (University of Freiburg, Southern University of Science and Technology) and Melissa Ruiz-Vasquez (University of Freiburg) for downloading and preparing the data used in this study. We thank Carsten F. Dormann and Jasper Denissen for insightful discussions and comments during the development of the analysis.

340 R.O. and J.K. acknowledge support from the German Research Foundation (Emmy Noether Grant No. 391059971). A.F.F. was supported by a NASA ECOSTRESS grant and NASA Terrestrial Ecology scoping study for a dryland field campaign, D.G.M. acknowledges the support of the ERC via the HEAT Consolidator grant (101088405).



## References

- AghaKouchak, A., Chiang, F., Huning, L. S., Love, C. A., Mallakpour, I., Mazdiyasni, O., Moftakhari, H., Papalexiou, S. M., Ragno, E.,  
 345 and Sadegh, M.: Climate Extremes and Compound Hazards in a Warming World, *Annual Review of Earth and Planetary Sciences*, 48,  
 519–548, <https://doi.org/10.1146/annurev-earth-071719-055228>, 2020.
- Alkama, R. and Cescatti, A.: Biophysical climate impacts of recent changes in global forest cover, *Science*, 351, 600–604,  
<https://doi.org/10.1126/science.aac8083>, publisher: American Association for the Advancement of Science, 2016.
- Allen, R. G., Pereira, L. S., Raes, D., and Smith, M.: Chapter 1 - Introduction to evapotranspiration, in: *Crop evapotranspiration - Guidelines*  
 350 *for computing crop water requirements*, FAO - Food and Agriculture Organization of the United Nations, [https://www.fao.org/4/x0490e/](https://www.fao.org/4/x0490e/x0490e00.htm#Contents)  
[x0490e00.htm#Contents](https://www.fao.org/4/x0490e/x0490e00.htm#Contents), 1998.
- Barriopedro, D., García-Herrera, R., Ordóñez, C., Miralles, D. G., and Salcedo-Sanz, S.: Heat Waves: Physical Understand-  
 ing and Scientific Challenges, *Reviews of Geophysics*, 61, e2022RG000780, <https://doi.org/10.1029/2022RG000780>, \_eprint:  
<https://onlinelibrary.wiley.com/doi/pdf/10.1029/2022RG000780>, 2023.
- 355 Bastos, A., Fu, Z., Ciais, P., Friedlingstein, P., Sitch, S., Pongratz, J., Weber, U., Reichstein, M., Anthoni, P., Arneth, A., Haverd, V., Jain, A.,  
 Joetzer, E., Knauer, J., Lienert, S., Loughran, T., McGuire, P. C., Obermeier, W., Padrón, R. S., Shi, H., Tian, H., Viovy, N., and Zaehle,  
 S.: Impacts of extreme summers on European ecosystems: a comparative analysis of 2003, 2010 and 2018, *Philosophical Transactions of*  
*the Royal Society B: Biological Sciences*, 375, 20190507, <https://doi.org/10.1098/rstb.2019.0507>, publisher: Royal Society, 2020.
- Benson, D. O. and Dirmeyer, P. A.: Characterizing the Relationship between Temperature and Soil Moisture Extremes and Their Role in the  
 360 Exacerbation of Heat Waves over the Contiguous United States, *Journal of Climate*, 34, 2175–2187, [https://doi.org/10.1175/JCLI-D-20-](https://doi.org/10.1175/JCLI-D-20-0440.1)  
 0440.1, publisher: American Meteorological Society Section: Journal of Climate, 2021.
- Brunner, L., Hegerl, G. C., and Steiner, A. K.: Connecting Atmospheric Blocking to European Temperature Extremes in Spring, *Journal*  
*of Climate*, 30, 585–594, <https://doi.org/10.1175/JCLI-D-16-0518.1>, publisher: American Meteorological Society Section: Journal of  
 Climate, 2017.
- 365 Brunner, L., Schaller, N., Anstey, J., Sillmann, J., and Steiner, A. K.: Dependence of Present and Future European Temperature Extremes on  
 the Location of Atmospheric Blocking, *Geophysical Research Letters*, 45, 6311–6320, <https://doi.org/10.1029/2018GL077837>, \_eprint:  
<https://onlinelibrary.wiley.com/doi/pdf/10.1029/2018GL077837>, 2018.
- Cheng, L., Zhang, L., Wang, Y.-P., Canadell, J. G., Chiew, F. H. S., Beringer, J., Li, L., Miralles, D. G., Piao, S., and Zhang, Y.: Recent  
 increases in terrestrial carbon uptake at little cost to the water cycle, *Nature Communications*, 8, 110, [https://doi.org/10.1038/s41467-017-](https://doi.org/10.1038/s41467-017-00114-5)  
 370 00114-5, publisher: Nature Publishing Group, 2017.
- Christian, J. I., Basara, J. B., Hunt, E. D., Otkin, J. A., and Xiao, X.: Flash drought development and cascading impacts associated with the  
 2010 Russian heatwave, *Environmental Research Letters*, 15, 094078, <https://doi.org/10.1088/1748-9326/ab9faf>, 2020.
- Collazo, S., Suli, S., Zaninelli, P. G., García-Herrera, R., Barriopedro, D., and Garrido-Perez, J. M.: Influence of large-scale circu-  
 lation and local feedbacks on extreme summer heat in Argentina in 2022/23, *Communications Earth & Environment*, 5, 1–17,  
 375 <https://doi.org/10.1038/s43247-024-01386-8>, publisher: Nature Publishing Group, 2024.
- De Boeck, H. J. and Verbeeck, H.: Drought-associated changes in climate and their relevance for ecosystem experiments and models,  
*Biogeosciences*, 8, 1121–1130, <https://doi.org/10.5194/bg-8-1121-2011>, publisher: Copernicus GmbH, 2011.



- Denissen, J. M. C., Teuling, A. J., Koirala, S., Reichstein, M., Balsamo, G., Vogel, M. M., Yu, X., and Orth, R.: Intensified future heat extremes linked with increasing ecosystem water limitation, *Earth System Dynamics*, 15, 717–734, [https://doi.org/10.5194/esd-15-717-](https://doi.org/10.5194/esd-15-717-2024)  
 380 2024, publisher: Copernicus GmbH, 2024.
- Duku, C. and Hein, L.: The impact of deforestation on rainfall in Africa: a data-driven assessment, *Environmental Research Letters*, 16, 064 044, <https://doi.org/10.1088/1748-9326/abfcfb>, publisher: IOP Publishing, 2021.
- Dunn, R. J. H., Alexander, L. V., Donat, M. G., Zhang, X., Bador, M., Herold, N., Lippmann, T., Allan, R., Aguilar, E., Barry, A. A., Brunet, M., Caesar, J., Chagnaud, G., Cheng, V., Cinco, T., Durre, I., de Guzman, R., Htay, T. M., Wan Ibadullah, W. M.,  
 385 Bin Ibrahim, M. K. I., Khoshkam, M., Kruger, A., Kubota, H., Leng, T. W., Lim, G., Li-Sha, L., Marengo, J., Mbatha, S., McGree, S., Menne, M., de los Milagros Skansi, M., Ngwenya, S., Nkrumah, F., Oonariya, C., Pabon-Caicedo, J. D., Panthou, G., Pham, C., Rahimzadeh, F., Ramos, A., Salgado, E., Salinger, J., Sané, Y., Sopaheluwakan, A., Srivastava, A., Sun, Y., Timbal, B., Trachow, N., Trewin, B., van der Schrier, G., Vazquez-Aguirre, J., Vasquez, R., Villarroel, C., Vincent, L., Vischel, T., Vose, R., and Bin Hj Yussof, M. N.: Development of an Updated Global Land In Situ-Based Data Set of Temperature and Precipitation Ex-  
 390 tremes: HadEX3, *Journal of Geophysical Research: Atmospheres*, 125, e2019JD032 263, <https://doi.org/10.1029/2019JD032263>, <https://agupubs.onlinelibrary.wiley.com/doi/pdf/10.1029/2019JD032263>, 2020.
- Feldman, A. F., Short Gianotti, D. J., Dong, J., Akbar, R., Crow, W. T., McColl, K. A., Konings, A. G., Nippert, J. B., Tumber-Dávila, S. J., Holbrook, N. M., Rockwell, F. E., Scott, R. L., Reichle, R. H., Chatterjee, A., Joiner, J., Poulter, B., and Entekhabi, D.: Remotely Sensed Soil Moisture Can Capture Dynamics Relevant to Plant Water Uptake, *Water Resources Research*, 59, e2022WR033 814,  
 395 <https://doi.org/10.1029/2022WR033814>, [eprint: https://agupubs.onlinelibrary.wiley.com/doi/pdf/10.1029/2022WR033814](https://agupubs.onlinelibrary.wiley.com/doi/pdf/10.1029/2022WR033814), 2023.
- Fischer, E. M., Rajczak, J., and Schär, C.: Changes in European summer temperature variability revisited, *Geophysical Research Letters*, 39, <https://doi.org/10.1029/2012GL052730>, [eprint: https://onlinelibrary.wiley.com/doi/pdf/10.1029/2012GL052730](https://onlinelibrary.wiley.com/doi/pdf/10.1029/2012GL052730), 2012.
- Garrido-Perez, J. M., Vicente-Serrano, S. M., Barriopedro, D., García-Herrera, R., Trigo, R., and Beguería, S.: Examining the outstanding Euro-Mediterranean drought of 2021–2022 and its historical context, *Journal of Hydrology*, 630, 130 653,  
 400 <https://doi.org/10.1016/j.jhydrol.2024.130653>, 2024.
- Gerken, T., Bromley, G. T., Ruddell, B. L., Williams, S., and Stoy, P. C.: Convective suppression before and during the United States Northern Great Plains flash drought of 2017, *Hydrology and Earth System Sciences*, 22, 4155–4163, <https://doi.org/10.5194/hess-22-4155-2018>, publisher: Copernicus GmbH, 2018.
- Gu, L., Schumacher, D. L., Fischer, E. M., Slater, L. J., Yin, J., Sippel, S., Chen, J., Liu, P., and Knutti, R.: Flash drought impacts on  
 405 global ecosystems amplified by extreme heat, *Nature Geoscience*, pp. 1–7, <https://doi.org/10.1038/s41561-025-01719-y>, publisher: Nature Publishing Group, 2025.
- Hansen, M.: Vegetation Continuous Fields, <https://doi.org/https://doi.org/10.5067/MEaSURES/VCF/VCF5KYR.001>.
- Hersbach, H., Bell, B., Berrisford, P., Hirahara, S., Horányi, A., Muñoz-Sabater, J., Nicolas, J., Peubey, C., Radu, R., Schepers, D., Simons, A., Soci, C., Abdalla, S., Abellan, X., Balsamo, G., Bechtold, P., Biavati, G., Bidlot, J., Bonavita, M., De Chiara, G., Dahlgren, P., Dee, D., Diamantakis, M., Dragani, R., Flemming, J., Forbes, R., Fuentes, M., Geer, A., Haimberger, L., Healy, S., Hogan, R. J., Hólm, E., Janisková, M., Keeley, S., Laloyaux, P., Lopez, P., Lupu, C., Radnoti, G., de Rosnay, P., Rozum, I., Vamborg, F., Villaume, S., and Thépaut, J.-N.: The ERA5 global reanalysis, *Quarterly Journal of the Royal Meteorological Society*, 146, 1999–2049,  
 410 <https://doi.org/10.1002/qj.3803>, [eprint: https://onlinelibrary.wiley.com/doi/pdf/10.1002/qj.3803](https://onlinelibrary.wiley.com/doi/pdf/10.1002/qj.3803), 2020.



- Hirschi, M., Seneviratne, S. I., Alexandrov, V., Boberg, F., Boroneant, C., Christensen, O. B., Formayer, H., Orlowsky, B., and  
 415 Stepanek, P.: Observational evidence for soil-moisture impact on hot extremes in southeastern Europe, *Nature Geoscience*, 4, 17–21,  
<https://doi.org/10.1038/ngeo1032>, publisher: Nature Publishing Group, 2011.
- Keenan, T. F., Hollinger, D. Y., Bohrer, G., Dragoni, D., Munger, J. W., Schmid, H. P., and Richardson, A. D.: Increase in forest water-  
 use efficiency as atmospheric carbon dioxide concentrations rise, *Nature*, 499, 324–327, <https://doi.org/10.1038/nature12291>, publisher:  
 Nature Publishing Group, 2013.
- 420 Kimutai, J., Barnes, C., Zachariah, M., Philip, S. Y., Kew, S. F., Pinto, I., Wolski, P., Koren, G., Vecchi, G., Yang, W., Li, S.,  
 Vahlberg, M., Singh, R., Heinrich, D., Arrighi, J., Marghidan, C. P., Thalheimer, L., Kane, C., Raju, E., and Otto, F. E. L.: Human-  
 induced climate change increased 2021–2022 drought severity in horn of Africa, *Weather and Climate Extremes*, 47, 100745,  
<https://doi.org/10.1016/j.wace.2025.100745>, 2025.
- Leeper, R. D., Harrington, T., Palecki, M. A., DePolt, K., Scott, E., Runkle, J., and Diamond, H. J.: The Influence of Drought on Heat Wave  
 425 Intensity, Duration, and Exposure, *Journal of Applied Meteorology and Climatology*, 64, 425–438, <https://doi.org/10.1175/JAMC-D-24-0072.1>, publisher: American Meteorological Society Section: Journal of Applied Meteorology and Climatology, 2025.
- Leite-Filho, A. T., Soares-Filho, B. S., Davis, J. L., Abrahão, G. M., and Börner, J.: Deforestation reduces rainfall and agricultural revenues  
 in the Brazilian Amazon, *Nature Communications*, 12, 2591, <https://doi.org/10.1038/s41467-021-22840-7>, publisher: Nature Publishing  
 Group, 2021.
- 430 Li, W., Migliavacca, M., Forkel, M., Denissen, J. M. C., Reichstein, M., Yang, H., Duveiller, G., Weber, U., and Orth, R.: Widespread  
 increasing vegetation sensitivity to soil moisture, *Nature Communications*, 13, 3959, <https://doi.org/10.1038/s41467-022-31667-9>, pub-  
 lisher: Nature Publishing Group, 2022.
- Manning, C., Widmann, M., Bevacqua, E., Van Loon, A. F., Maraun, D., and Vrac, M.: Increased probability of compound long-duration  
 dry and hot events in Europe during summer (1950–2013), *Environmental Research Letters*, 14, 094006, <https://doi.org/10.1088/1748-9326/ab23bf>, 2019.
- 435 Marchin, R. M., Backes, D., Ossola, A., Leishman, M. R., Tjoelker, M. G., and Ellsworth, D. S.: Extreme heat increases stomatal conductance  
 and drought-induced mortality risk in vulnerable plant species, *Global Change Biology*, 28, 1133–1146, <https://doi.org/10.1111/gcb.15976>,  
 \_eprint: <https://onlinelibrary.wiley.com/doi/pdf/10.1111/gcb.15976>, 2022.
- Michaelian, M., Hogg, E. H., Hall, R. J., and Arsenault, E.: Massive mortality of aspen following severe drought along the southern  
 440 edge of the Canadian boreal forest, *Global Change Biology*, 17, 2084–2094, <https://doi.org/10.1111/j.1365-2486.2010.02357.x>, \_eprint:  
<https://onlinelibrary.wiley.com/doi/pdf/10.1111/j.1365-2486.2010.02357.x>, 2011.
- Miralles, D. G., Teuling, A. J., van Heerwaarden, C. C., and Vilà-Guerau de Arellano, J.: Mega-heatwave temperatures due to combined soil  
 desiccation and atmospheric heat accumulation, *Nature Geoscience*, 7, 345–349, <https://doi.org/10.1038/ngeo2141>, number: 5 Publisher:  
 Nature Publishing Group, 2014.
- 445 Miralles, D. G., Gentile, P., Seneviratne, S. I., and Teuling, A. J.: Land–atmospheric feedbacks during droughts and heatwaves: state of the  
 science and current challenges, *Annals of the New York Academy of Sciences*, 1436, 19–35, <https://doi.org/10.1111/nyas.13912>, 2019.
- Miralles, D. G., Bonte, O., Koppa, A., Baez-Villanueva, O. M., Tronquo, E., Zhong, F., Beck, H. E., Hulsman, P., Dorigo, W., Verhoest,  
 N. E. C., and Haghdoust, S.: GLEAM4: global land evaporation and soil moisture dataset at 0.1° resolution from 1980 to near present,  
*Scientific Data*, 12, 416, <https://doi.org/10.1038/s41597-025-04610-y>, publisher: Nature Publishing Group, 2025.



- 450 Mueller, B. and Seneviratne, S. I.: Hot days induced by precipitation deficits at the global scale, *Proceedings of the National Academy of Sciences*, 109, 12 398–12 403, <https://doi.org/10.1073/pnas.1204330109>, publisher: Proceedings of the National Academy of Sciences, 2012.
- Muñoz-Sabater, J., Dutra, E., Agustí-Panareda, A., Albergel, C., Arduini, G., Balsamo, G., Boussetta, S., Choulga, M., Harrigan, S., Hersbach, H., Martens, B., Miralles, D. G., Piles, M., Rodríguez-Fernández, N. J., Zsoter, E., Buontempo, C., and Thépaut, J.-N.: ERA5-Land:  
 455 a state-of-the-art global reanalysis dataset for land applications, *Earth System Science Data*, 13, 4349–4383, <https://doi.org/10.5194/essd-13-4349-2021>, publisher: Copernicus GmbH, 2021.
- Nelson, J. A., Walther, S., Gans, F., Kraft, B., Weber, U., Novick, K., Buchmann, N., Migliavacca, M., Wohlfahrt, G., Šigut, L., Ibrom, A., Papale, D., Göckede, M., Duveiller, G., Knohl, A., Hörtnagl, L., Scott, R. L., Dušek, J., Zhang, W., Hamdi, Z. M., Reichstein, M., Aranda-Barranco, S., Ardö, J., Op de Beeck, M., Billesbach, D., Bowling, D., Bracho, R., Brümmer, C., Camps-Valls, G., Chen, S., Cleverly, J. R.,  
 460 Desai, A., Dong, G., El-Madany, T. S., Euskirchen, E. S., Feigenwinter, I., Galvagno, M., Gerosa, G. A., Gielen, B., Goded, I., Goslee, S., Gough, C. M., Heinesch, B., Ichii, K., Jackowicz-Korczynski, M. A., Klosterhalfen, A., Knox, S., Kobayashi, H., Kohonen, K.-M., Korkiakoski, M., Mammarella, I., Gharun, M., Marzuoli, R., Matamala, R., Metzger, S., Montagnani, L., Nicolini, G., O'Halloran, T., Ourcival, J.-M., Peichl, M., Pendall, E., Ruiz Reverter, B., Roland, M., Sabbatini, S., Sachs, T., Schmidt, M., Schwalm, C. R., Shekhar, A., Silberstein, R., Silveira, M. L., Spano, D., Tagesson, T., Tramontana, G., Trotta, C., Turco, F., Vesala, T., Vincke, C., Vitale, D., Vivoni,  
 465 E. R., Wang, Y., Woodgate, W., Yezpe, E. A., Zhang, J., Zona, D., and Jung, M.: X-BASE: the first terrestrial carbon and water flux products from an extended data-driven scaling framework, *FLUXCOM-X, Biogeosciences*, 21, 5079–5115, <https://doi.org/10.5194/bg-21-5079-2024>, publisher: Copernicus GmbH, 2024.
- O, S. and Orth, R.: Global soil moisture data derived through machine learning trained with in-situ measurements, *Scientific Data*, 8, 170, <https://doi.org/10.1038/s41597-021-00964-1>, 2021.
- 470 O, S., Bastos, A., Reichstein, M., Li, W., Denissen, J., Graefen, H., and Orth, R.: The Role of Climate and Vegetation in Regulating Drought–Heat Extremes, *Journal of Climate*, 35, 5677–5685, <https://doi.org/10.1175/JCLI-D-21-0675.1>, publisher: American Meteorological Society Section: Journal of Climate, 2022.
- Rasmijn, L. M., van der Schrier, G., Bintanja, R., Barkmeijer, J., Sterl, A., and Hazeleger, W.: Future equivalent of 2010 Russian heatwave intensified by weakening soil moisture constraints, *Nature Climate Change*, 8, 381–385, <https://doi.org/10.1038/s41558-018-0114-0>, publisher: Nature Publishing Group, 2018.
- Russo, A., Gouveia, C. M., Dutra, E., Soares, P. M. M., and Trigo, R. M.: The synergy between drought and extremely hot summers in the Mediterranean, *Environmental Research Letters*, 14, 014 011, <https://doi.org/10.1088/1748-9326/aaf09e>, publisher: IOP Publishing, 2019.
- Schumacher, D. L., Keune, J., Van Heerwaarden, C. C., Vilà-Guerau De Arellano, J., Teuling, A. J., and Miralles, D. G.: Amplification of mega-heatwaves through heat torrents fuelled by upwind drought, *Nature Geoscience*, 12, 712–717, <https://doi.org/10.1038/s41561-019-0431-6>, 2019.  
 480
- Seneviratne, S. I., Lüthi, D., Litschi, M., and Schär, C.: Land–atmosphere coupling and climate change in Europe, *Nature*, 443, 205–209, <https://doi.org/10.1038/nature05095>, publisher: Nature Publishing Group, 2006.
- Seneviratne, S. I., Corti, T., Davin, E. L., Hirschi, M., Jaeger, E. B., Lehner, I., Orlowsky, B., and Teuling, A. J.: Investigating soil moisture–climate interactions in a changing climate: A review, *Earth-Science Reviews*, 99, 125–161, <https://doi.org/10.1016/j.earscirev.2010.02.004>, 2010.  
 485
- Seneviratne, S.I., Zhang, X., Adnan, M., Badi, W., Dereczynski, C., Di Luca, A., Ghosh, S., Iskandar, I., Kossin, J., Lewis, S., Otto, F., Pinto, I., Satoh, M., Vicente-Serrano, S.M., Wehner, M., and Zhou, B.: Weather and Climate Extreme Events in a Changing Climate, in: *Climate*





- Change 2021 – The Physical Science Basis: Working Group I Contribution to the Sixth Assessment Report of the Intergovernmental Panel on Climate Change, Cambridge University Press, 1 edn., ISBN 978-1-00-915789-6, <https://doi.org/10.1017/9781009157896>, 2023.
- 490 Stegehuis, A. I., Vautard, R., Ciais, P., Teuling, A. J., Jung, M., and Yiou, P.: Summer temperatures in Europe and land heat fluxes in observation-based data and regional climate model simulations, *Climate Dynamics*, 41, 455–477, <https://doi.org/10.1007/s00382-012-1559-x>, 2013.
- Teuling, A. J.: A hot future for European droughts, *Nature Climate Change*, 8, 364–365, <https://doi.org/10.1038/s41558-018-0154-5>, publisher: Nature Publishing Group, 2018.
- 495 Teuling, A. J., Van Loon, A. F., Seneviratne, S. I., Lehner, I., Aubinet, M., Heinesch, B., Bernhofer, C., Grünwald, T., Prasse, H., and Spank, U.: Evapotranspiration amplifies European summer drought, *Geophysical Research Letters*, 40, 2071–2075, <https://doi.org/10.1002/grl.50495>, \_eprint: <https://agupubs.onlinelibrary.wiley.com/doi/pdf/10.1002/grl.50495>, 2013.
- Thom, D., Buras, A., Heym, M., Klemmt, H.-J., and Wauer, A.: Varying growth response of Central European tree species to the extraordinary drought period of 2018 – 2020, *Agricultural and Forest Meteorology*, 338, 109 506, <https://doi.org/10.1016/j.agrformet.2023.109506>,  
 500 2023.
- Uckan, Y., Ruiz-Vázquez, M., De Polt, K., and Orth, R.: Global relevance of atmospheric and land surface drivers for hot temperature extremes, *Earth System Dynamics*, 16, 869–889, <https://doi.org/10.5194/esd-16-869-2025>, publisher: Copernicus GmbH, 2025.
- Vicente-Serrano, S. M., McVicar, T. R., Miralles, D. G., Yang, Y., and Tomas-Burguera, M.: Unraveling the influence of atmospheric evaporative demand on drought and its response to climate change, *WIREs Climate Change*, 11, e632, <https://doi.org/10.1002/wcc.632>, \_eprint: <https://wires.onlinelibrary.wiley.com/doi/pdf/10.1002/wcc.632>, 2020.
- 505 Vogel, M. M., Orth, R., Cheruy, F., Hagemann, S., Lorenz, R., van den Hurk, B. J. J. M., and Seneviratne, S. I.: Regional amplification of projected changes in extreme temperatures strongly controlled by soil moisture-temperature feedbacks, *Geophysical Research Letters*, 44, 1511–1519, <https://doi.org/10.1002/2016GL071235>, \_eprint: <https://onlinelibrary.wiley.com/doi/pdf/10.1002/2016GL071235>, 2017.
- Vogel, M. M., Zscheischler, J., and Seneviratne, S. I.: Varying soil moisture–atmosphere feedbacks explain divergent temperature extremes and precipitation projections in central Europe, *Earth System Dynamics*, 9, 1107–1125, <https://doi.org/10.5194/esd-9-1107-2018>, publisher: Copernicus GmbH, 2018.
- Whan, K., Zscheischler, J., Orth, R., Shongwe, M., Rahimi, M., Asare, E. O., and Seneviratne, S. I.: Impact of soil moisture on extreme maximum temperatures in Europe, *Weather and Climate Extremes*, 9, 57–67, <https://doi.org/10.1016/j.wace.2015.05.001>, 2015.
- Xu, R., Li, Y., Teuling, A. J., Zhao, L., Spracklen, D. V., Garcia-Carreras, L., Meier, R., Chen, L., Zheng, Y., Lin, H., and Fu, B.: Contrasting  
 515 impacts of forests on cloud cover based on satellite observations, *Nature Communications*, 13, 670, <https://doi.org/10.1038/s41467-022-28161-7>, publisher: Nature Publishing Group, 2022.
- Xu, Y., Lamarque, J.-F., and Sanderson, B. M.: The importance of aerosol scenarios in projections of future heat extremes, *Climatic Change*, 146, 393–406, <https://doi.org/10.1007/s10584-015-1565-1>, 2018.
- Yin, D., Roderick, M. L., Leech, G., Sun, F., and Huang, Y.: The contribution of reduction in evaporative cooling to higher surface air temperatures during drought, *Geophysical Research Letters*, 41, 7891–7897, <https://doi.org/10.1002/2014GL062039>, \_eprint: <https://onlinelibrary.wiley.com/doi/pdf/10.1002/2014GL062039>, 2014.
- 520 Zha, T., Barr, A. G., van der Kamp, G., Black, T. A., McCaughey, J. H., and Flanagan, L. B.: Interannual variation of evapotranspiration from forest and grassland ecosystems in western canada in relation to drought, *Agricultural and Forest Meteorology*, 150, 1476–1484, <https://doi.org/10.1016/j.agrformet.2010.08.003>, 2010.



- 525 Zhao, A., Bollasina, M. A., and Stevenson, D. S.: Strong Influence of Aerosol Reductions on Future Heatwaves, *Geophysical Research Letters*, 46, 4913–4923, <https://doi.org/10.1029/2019GL082269>, \_eprint: <https://onlinelibrary.wiley.com/doi/pdf/10.1029/2019GL082269>, 2019.
- Zou, Y., Macau, E. E. N., Sampaio, G., Ramos, A. M. T., and Kurths, J.: Characterizing the exceptional 2014 drought event in São Paulo by drought period length, *Climate Dynamics*, 51, 433–442, <https://doi.org/10.1007/s00382-017-3932-2>, 2018.
- 530 Zscheischler, J., Orth, R., and Seneviratne, S. I.: A submonthly database for detecting changes in vegetation-atmosphere coupling, *Geophysical Research Letters*, 42, 9816–9824, <https://doi.org/10.1002/2015GL066563>, \_eprint: <https://onlinelibrary.wiley.com/doi/pdf/10.1002/2015GL066563>, 2015.